Editor: Liquan Xie

Applied Mechanics and Civil Engineering VI

CRC Press
Taylor & Francis Group
A BALKEMA BOOK

APPLIED MECHANICS AND CIVIL ENGINEERING VI

PROCEEDINGS OF THE 6TH INTERNATIONAL CONFERENCE ON APPLIED MECHANICS AND CIVIL ENGINEERING (AMCE 2016), HONG KONG, 30–31 DECEMBER 2016

Applied Mechanics and Civil Engineering VI

Editor

Liquan Xie

Department of Hydraulic Engineering, Tongji University, China

CRC Press
Taylor & Francis Group
Boca Raton London New York Leiden

CRC Press is an imprint of the
Taylor & Francis Group, an **informa** business
A BALKEMA BOOK

CRC Press/Balkema is an imprint of the Taylor & Francis Group, an informa business

Typeset by V Publishing Solutions Pvt Ltd., Chennai, India
Printed and bound in Great Britain and USA

Published by: CRC Press/Balkema
P.O. Box 11320, 2301 EH Leiden, The Netherlands
e-mail: Pub.NL@taylorandfrancis.com
www.crcpress.com – www.taylorandfrancis.com

ISBN: 978-1-138-62631-7 (Hbk)
ISBN: 978-1-315-22907-2 (eBook)

Applied Mechanics and Civil Engineering VI – Xie (Ed.)
© 2017 Taylor & Francis Group, London, ISBN 978-1-138-62631-7

Table of contents

Applied Mechanics and Civil Engineering VI – Xie (Ed.)
© 2017 Taylor & Francis Group, London, ISBN 978-1-138-62631-7

Preface

Applied Mechanics and Civil Engineering VI includes the selected, peer reviewed papers that will be presented at the 6th International Conference on Applied Mechanics and Civil Engineering (AMCE 2016). AMCE 2016 showcases the exciting and challenging developments occurring in the area of applied mechanics, civil engineering and associated engineering practice, and serves as a major forum for researchers, engineers and manufacturers to share recent advances, discuss problems, and identify practical challenges associated with the engineering applications. The contributions from experts and world-renowned scientists cover a wide variety of topics:

– Applied mechanics and its applications in civil engineering;
– Bridge engineering;
– Underground engineering;
– Structural safety and reliability;
– Reinforced concrete (RC) structures;
– Rock mechanics and rock engineering;
– Geotechnical in-situ testing & monitoring;
– New construction materials and applications;
– Computational mechanics;
– Natural hazards and risk, and
– Water and hydraulic engineering.

Applied Mechanics and Civil Engineering VI will appeal to professionals and academics involved in the above mentioned areas. Although these papers represent only modest advances toward overcoming major scientific problems in civil engineering, some of the technologies might be key factors in the success of future engineering advances. It is expected that this book will stimulate new ideas, methods and applications in ongoing civil engineering advances.

We would like to express our deep gratitude to all authors, reviewers for their excellent work, and Léon Bijnsdorp, Lukas Goosen and other editors from Taylor & Francis Group for their wonderful work.

Applied Mechanics and Civil Engineering VI – Xie (Ed.)
 ISBN 978-1-138-62631-7

Behavior of large deformation and supporting measures in soft rock tunnel

Kang Bian
State Key Laboratory of Geomechanics and Geotechnical Engineering, Institute of Rock and Soil Mechanics, Chinese Academy of Science, Wuhan, Hubei Province, P.R. China

Xiaoqing Zheng
State Key Laboratory of Geomechanics and Geotechnical Engineering, Institute of Rock and Soil Mechanics, Chinese Academy of Science, Wuhan, Hubei Province, P.R. China
University of Chinese Academy of Sciences, Beijing, P.R. China

Yuwei He
Hubei Wuxue Yangtze River Highway Bridge Co. Ltd., Wuxue, Hubei Province, P.R. China

Jian Liu
State Key Laboratory of Geomechanics and Geotechnical Engineering, Institute of Rock and Soil Mechanics, Chinese Academy of Science, Wuhan, Hubei Province, P.R. China

ABSTRACT: Typical large-deformation phenomena of soft rock occurred frequently during tunneling in Huangjiazhai Tunnel. The monitoring results indicated that the deformation had the characteristics of large magnitude, high velocity, long duration and inhomogeneity of spatial distribution. The results of in-situ stress test showed that, as a result of high tectonic stress and lower rock strength, the drilling test area of tunnel was regarded as extremely-high stress area, even if the maximum buried depth (270 m) of tunnel was not too large. Based on the New Austrian Tunneling Method, new comprehensive supporting measures were utilized in Huangjiazhai Tunnel, which were consisted of increase of the reserved deformation, bolt and grouting supporting, accelerating the construction of inverted arch and secondary lining and adjusting the spacing and type of steel arch. It was proved in the subsequent construction that the above supporting design was effective for controlling the large deformation in Huangjiazhai Tunnel.

1 INTRODUCTION

A large number of highways run across the mountains in the central and western regions of China, therefore, tunnel engineering plays a significant role in the highway construction. Due to the complex topographic and geological conditions, large deformation phenomena in soft rock tunnels are frequently encountered, which induce different degrees of damage of primary support and secondary lining. More seriously, severe extrusion induced by large deformation commonly leads to instability of tunnel, resulting in significant difficulties in tunnel design and construction. Consequently, the proper supporting measures applied in large-deformation tunnels are of importance to complete the constructions safely.

Studies on deformation behavior and supporting measures in soft rock tunnel have been conducted by a large number of researchers (He Manchao et al., 2002, 2013; Li Hongbo et al., 2011; Liu Gao et al., 2005; Dai Yonghao et al., 2015; Karmen F.B. et al., 2004). He Manchao et al. (2002, 2013) proposed an initiative supporting technology system which was based on constant resistance with large deformation coupling support. Liu Gao et al. (2005) researched the intense deformation and serious failure in Muzhailing tunnel, and proposed the mechanism of large deformation in this tunnel. Li Hongbo et al. (2011) studied the monitoring results of deformation and structural stress for Xiakou soft rock tunnel. Dai Yonghao et al. (2015) presented comprehensive support measures in Daliang tunnel which suffered large deformation. Nevertheless, the existing researches are lacking of combining analysis of the behavior of large deformation, the geostress results and supporting measures in soft rock tunnel. In this paper, taking an example of Huangjiazhai Tunnel in Northwest Hubei Province, the large-deformation characteristics are summarized. And then, combining the in-situ stress test and laboratory experiments, the cause of large deformation is analyzed. Finally, new comprehensive supporting measures were proposed and utilized, which were proved effectively for controlling the large deformation in the subsequent construction in Huangjiazhai Tunnel.

2 PROJECT OVERVIEW

Huangjiazhai Tunnel is one of 29 tunnels of Macheng-Zhuxi Highway, which is located at north-west of Hubei province in Central China. Designed as a long separated tunnel, Huangjiazhai Tunnel has the maximum buried depth of 270 m, with the whole length of 1437 m. Both of the two tunnels are of 12.4 m width and 9.9 m height, and the end-wall portal form is chosen. The tunnel sites are mainly hilly areas, also including small amounts of valleys and terraces. Both the entrances and exits of the tunnel are situated at the halfway up the hills, and the slope angles are mostly between 15 degree and 20 degree.

The principal strata locating at the construction site of Huangjiazhai Tunnel is Silurian shale belonging to the Sllm Group (S_1l). Quaternary residual gravelly soil (Q_4^{el+dl}) composes the covering layer of this area. Geological explorations via boreholes drilled at the tunnel route show that three layers could be divided from the earth's surface to the bottom: gravelly soil, intense weathering shale and intermediary weathered shale. In general, the rock masses present mostly fragmentized, jointed and pelitic, with thin-layered structure.

The New Austrian Tunnelling Method (NATM) is applied in construction of Huangjiazhai Tunnel. At the regions where the rock masses are considered as grade V, the ring cut method is used; at the other parts, the bench cut method is utilized. The initial supports in the tunnel are combinative technologies, including rock bolt, steel arch support, reinforcing mesh and shotcrete. After that, the reinforced concrete is applied as the secondary lining.

3 LARGE-DEFORMATION PHENOMENA DURING TUNNELLING

During tunneling, typical large-deformation phenomena of soft rock occurred frequently in Huangjiazhai Tunnel, some of the examples are described as follows.

Fig. 1 shows the typical squeezing phenomenon of the sidewall. Affected by the collapse at the section between K60 + 733 and K60 + 734.2, severe deformation occurred at the section between K60 + 745 and K60 + 753 of the right tunnel. The primary support cracked and peeled off, with steel arch at the left sidewall distorted. More seriously, the primary support intruded into the outline of the secondary lining, the maximum intrusion value even reached 105.3 cm at the section K60 + 745. As a result, the primary support at the intrusion section should be chiseled off and replaced.

Collapse happened at the section between K60 + 733 and K60 + 734.2, as shown in Fig. 2. When the primary supports were chiseled off at the section between K60 + 733 and K60 + 734.2, some of the rock fragments slipped from the left sidewall and crown; and as time passed by, the amount of rock fragments increased rapidly, and collapse was induced.

Fig. 3 shows the cracking of secondary lining at the sidewall. The surface concrete gradually peeled off, and the reinforcement meshes were exposed at the section between ZK60 + 690.5 and ZK60 + 707. The above phenomena aggravated when the continuous raining days came.

The shotcrete cracking occurred at the entrance slope of right tunnel after continuous heavy rain, as shown in Fig. 4. Through uninterrupted observation, the width and extended length of the crack increasingly expanded as time went on, and the maximum values reached 40 cm and 15 m respectively. Finally, a through crack appeared, and the adjacent parts were at risk from

Figure 1. Squeezing of the sidewall.

Figure 2. Collapse inside the tunnel.

Figure 3. Cracking of secondary lining.

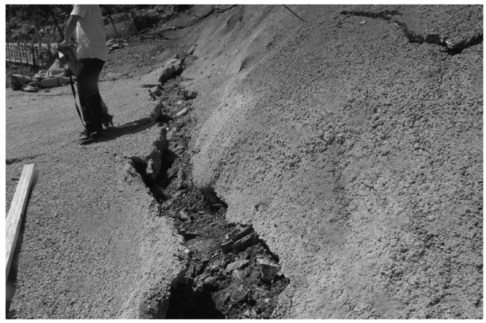

Figure 4. Shotcrete cracking at the entrance slope.

landslides. According to the monitoring results, the maximum velocity of surface subsidence at the entrance slope exceeded 16 mm/d, which accelerated the expansion of shotcrete crack.

4 MONITORING SITUATION

The monitoring results could present quantitative data to analyze the real situation during tunneling process at Huangjiazhai Tunnel. Fig. 5 and Fig. 6 show the monitoring results of horizontal convergence and crown settlement of four typical sections in Huangjiazhai Tunnel. Fig. 7 shows the monitoring results of surface subsidence at the entrance slope of right tunnel. In general, several characteristics of deformation in Huangjiazhai Tunnel could be summarized as follows.

1. The large accumulative deformation. According to the monitoring results, the accumulative horizontal displacement and crown settlement of all four sections exceeded 100 mm. At the zones where the surrounding rocks were loose and fragmentized, e.g. Section ZK60 + 645, the maximum horizontal displacement even exceeded 350 mm within 50 days, and the maximum crown settlement reached 314 mm. Besides, the accumulative surface subsidence at the entrance slope of right tunnel also reached 183 mm within 23 days.
2. The large deformation velocity, especially at the initial period. In the initial several days, the deformation velocity inside the tunnel remained at a high level; as time gone by, after the monitoring lasting for 3 to 5 days, the deformation velocity would decrease. The maximum velocity of horizontal convergence exceeded 24 mm/d at Section ZK60 + 750 when the monitoring lasted for three days, and the maximum velocity of crown settlement was 18 mm/d at the fourth day after monitoring.
3. The long duration of deformation. During the whole monitoring period (50 days), both the horizontal and vertical deformations of monitoring sections had no convergent tendency. In general, the monitoring results of deformation at Huangjiazhai Tunnel represented typical rheologic characteristics of surrounding rock.

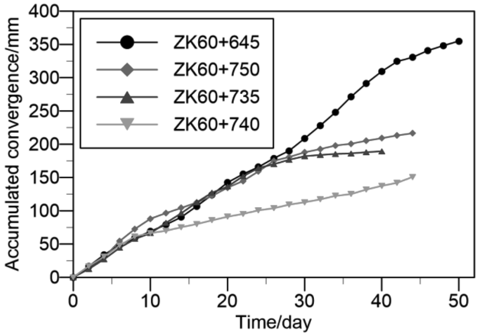

Figure 5. Curve between horizontal convergence and time of four sections in tunnel.

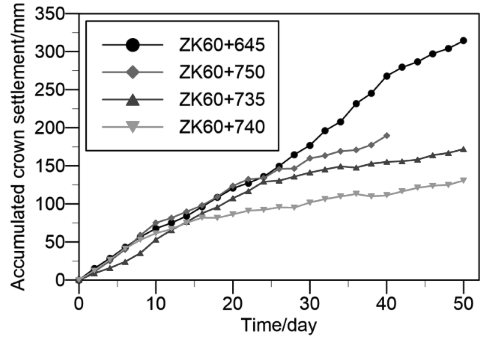

Figure 6. Curve between crown settlement and time of four sections in tunnel.

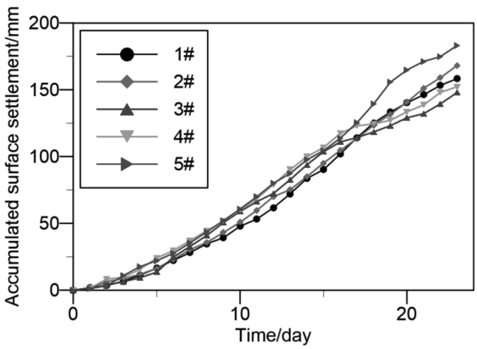

Figure 7. Curve between surface subsidence and time at the entrance slope of right tunnel.

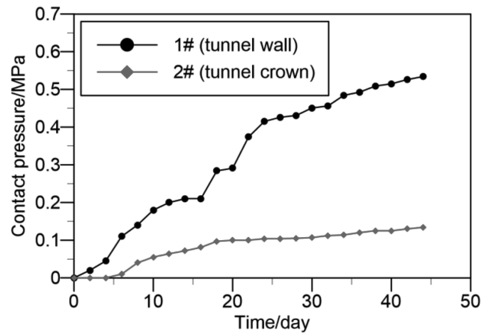

Figure 8. Curve between contact pressure and time at stake YK61+666.

4. The inhomogeneity of deformation distribution. Even though the displacements at Huangjiazhai Tunnel were generally large, the tunnel deformations were obviously much bigger at the fractured zones and the groundwater-developed zones than the other positions. Moreover, the horizontal displacements at most of monitoring sections were larger than the values of crown subsidence.

Fig. 8 shows the monitoring results of contact pressure between primary support and surrounding rock at stake YK61 + 666 in Huangjiazhai Tunnel. It was seen that during the observation period, the contact pressure kept a continuous increasing trend and had no convergent tendency within 43 days. Moreover, sudden increase of contact pressure occurred at the 18th and 22th day after monitoring, as a result of blasting disturbance at adjacent sections. From the point of view of magnitude, the pressure at tunnel wall was generally bigger than the value at arch crown; and the maximum contact pressure between primary support and surrounding rock reached 0.534 MPa.

5 GROUND STRESS TEST

The ground stress test was utilized to assess the geostress level at Huangjiazhai Tunnel. The vertical borehole for geostress measurement, with a depth of 50 m, was located at the stake YK61 + 195 in the right tunnel, and the buried depth of measurement part was 260 m. The hydraulic fracturing method was applied in the geostress test, and the results are listed in Table 1.

Table 1. Results of geostress test in vertical borehole at Huangjiazhai Tunnel.

Depth m	Maximum horizontal principal stress MPa	Minimum horizontal principal stress MPa	Vertical stress MPa	Direction of maximum horizontal principal stress
18	2.44	2.14	7.23	/
22	6.41	4.30	7.33	/
26	13.20	7.01	7.44	/
30	12.61	6.56	7.54	/
37	11.90	6.56	7.72	/
39	14.33	7.85	7.77	NE8°
41	14.60	7.86	7.83	NE10°

As shown in Table 1, within the depth range of geostress measurement, the maximum horizontal principal stress at the borehole is 14.60 MPa, and the direction of maximum horizontal principal stress is NE10°. The results indicate that the maximum principal stress and the second principal stress are both horizontal stresses, and only the minimum principal stress is vertical stress. Furthermore, the lateral pressure coefficient of geostress at the borehole, defined as the ratio of the maximum horizontal principal stress and the vertical stress, is nearly 1.8. Therefore, the tectonic stress is the primary composition of the geostress at the tunnel site. Consequently, a conclusion could be drawn that the region where Huangjiazhai Tunnel locates had experienced intense tectonic movements in the geological history, which could be also verified by the littery attitude of tunnel rock.

The grade of rock mass stresses could be defined by the ratio of uniaxial compressive strength to maximum principal stress, and it could be considered as extremely-high stress area when the ratio is less than 4. In fact, according to laboratory experiments, the uniaxial compressive strength of shale specimen taking from Huangjiazhai Tunnel is 23.3 MPa. Therefore, the ratio is only 1.6 at the borehole, which indicates that although the maximum buried depth (270 m) of tunnel is not too large, as a result of high tectonic stress and lower rock strength, the drilling test area of Huangjiazhai Tunnel is regarded as extremely-high stress area.

6 SUPPORTING MEASURES AGAINST LARGE DEFORMATION

Based on the above analysis, the squeezing deformation in Huangjiazhai tunnel may be due to the rheology of shale under extremely-high geostress, and the low strength and integrity of the rock masses constitute the basic conditions of large deformation.

According to the monitoring results, the deformation and contact pressure of surrounding rock in Huangjiazhai Tunnel changed typically over time, and the existing supporting design could not satisfy the demands of tunnel stability. Therefore, adjusted supporting design should be presented to adapt the special geological condition in Huangjiazhai Tunnel. Based on the New Austrian Tunneling Method, in the design of the primary support, a certain extent of deformation of surrounding rock induced by excavation is allowable, and then sufficient support should be applied in order to prevent the tunnel from buckling failure. The specific measures were listed as follows.

1. Reinforcement at the large deformation and cracking parts. The temporary steel support was utilized at the tunnel wall of large deformation parts, in order to provide resistance of creep deformation. To the cracking parts of primary support, grouting reinforcement in surrounding rock with perforated steel pipes was used.
2. Increase of the reserved deformation. The original reserved deformation was chosen as 12 cm, which was obviously less than the actual deformation monitored in Huangjiazhai Tunnel. To prevent the primary support intruding into the outline of the secondary

Table 2. Parameters of advance ductile grouting in the adjusted supporting design.

Diameter mm	Length m	Circumferential spacing cm	External angle °	Grouting pressure MPa
42	3.5	80~100	5~10	0.8

lining, as well as reduce the surrounding rock pressure borne by the secondary lining, the adjusted reserved deformation was chosen as 30 cm.

3. Bolt and grouting supporting. Since the rock mass exposing at the working face in Huangjiazhai Tunnel was more fragmentized and jointed than design, in order to increase the integrity and deformation resistance of surrounding rock, bolt and grouting supporting was necessary. At the fractured zones, the advance ductile grouting was utilized at the whole excavation section; and the proportion of cement and water was chosen as 1:1. The parameters of ductile grouting were shown in Table 2.
4. Accelerating the construction of inverted arch and secondary lining. To the squeezing tunnel, the secondary lining should not be applied until the deformation of primary support was completely stable. The inverted arch would be constructed as early as possible, and the construction of secondary lining would be carried out in time, immediately after the velocity of deformation reducing to 3~5 mm/d, in order to form the enclosed load-bearing ring and improve the structure stress of tunnel.
5. Adjusting the spacing and type of steel arch. To improve the capability of deformation resistance of steel support, the steel arch was more densely distributed with spacing of 50 mm instead of 60 mm; and moreover, the I20b I-steel was used, taking the place of the original type I18.

After the adjusted supporting design was carried out, the magnitude and velocity of tunnel deformation reduced significantly, according to the subsequent monitoring results. Furthermore, the incidence of large deformation phenomena, including squeezing of the sidewall and damage of the primary support, was decreasing in the following days. It was proved that the adjusted supporting design was effective for controlling the large deformation in Huangjiazhai Tunnel.

7 CONCLUSIONS

During tunneling, typical large-deformation phenomena of soft rock occurred frequently in Huangjiazhai Tunnel, e.g. squeezing of the sidewall, collapse inside the tunnel, severe cracking of secondary lining and shotcrete cracking at the entrance slope.

The monitoring results indicate that the deformation in Huangjiazhai Tunnel has the characteristics of large magnitude, high velocity, long duration and inhomogeneity of spatial distribution.

Based on the results of geostress test and laboratory experiment, although the maximum buried depth (270 m) of tunnel is not big enough, as a result of high tectonic stress and lower rock strength, the drilling test area of Huangjiazhai Tunnel is regarded as extremely-high stress area.

Adjusted support measures were represented and utilized in Huangjiazhai Tunnel, including the temporary steel support utilized at the tunnel wall of large deformation parts; increase of the reserved deformation; bolt and grouting supporting; accelerating the construction of inverted arch and secondary lining; adjusting the spacing and type of steel arch. It was proved in the subsequent construction that the above supporting design was effective for controlling the large deformation in Huangjiazhai Tunnel. It also provides feasible support measures against large deformation in squeezing tunnels, which could be referred in similar projects.

ACKNOWLEDGEMENT

The authors gratefully acknowledge the support by the National Key Research and Development Project of China (Grant No. 2016YFC0401802), the State Key Program of National Natural Science of China (Grant No. 51539002) and the National Natural Science Foundation of China (Nos. 51209198 and 51204158).

REFERENCES

Dai Yonghao, Chen Weizhong, Tian Hongming, et al. 2015. Study of Large Deformation and Support Measures of Daliang Tunnel with Soft Surrounding Rockmass. Chinese Journal of Rock Mechanics and Engineering 34(Supp.2): 4149–4156.

He Manchao, Jing Haihe, Sun Xiaoming. 2002. Engineering Mechanics of Soft Rock. Beijing: Science Press.

He Manchao, Yuan Yue, Wang Xiaolei, et al. 2013. Control technology for large deformation of Mesozoic compound soft rock in Xinjiang and its application. Chinese Journal of Rock Mechanics and Engineering 32(3): 433–441.

Karmen F.B., Borut P. 2004. Displacement analysis of tunnel support in soft rock around a shallow highway tunnel at Golovec. Engineering Geology 75: 89–106.

Li Hongbo, Dai Yonghao, Song Jihong, et al. 2011. Construction monitoring and support design of Xiakou tunnel under high stress with soft rock surrounding. Rock and Soil Mechanics 32(Supp.2): 496–501.

Liu Gao, Zhang Fanyu, Li Xinzhao, et al. 2005. Research on large deformation and its mechanism of Muzhailing tunnel. Chinese Journal of Rock Mechanics and Engineering 24(Supp.2): 5521–5526.

Applied Mechanics and Civil Engineering VI – Xie (Ed.)
 ISBN 978-1-138-62631-7

Integrating *in situ* tests on the excavation damaged zone of underground caverns

F. Ai & J. Liu
State Key Laboratory of Geomechanics and Geotechnical Engineering, Institute of Rock and Soil Mechanics, Chinese Academy of Science, Wuhan, Hubei Province, P.R. China

N.S. Chen
Northwest Engineering Corporation Limited, Power China, Xian, Shanxi Province, P.R. China

H.B. Xiao
Huaneng Lancang River Hydropower Corporation Limited, Kunming, Yunnan Province, P.R. China

G.H. Shao
Wulonglong and Lidi Hydropower Construction Authority, Huaneng Lancang River Hydropower Corporation Limited, Kunming, Yunnan Province, P.R. China

ABSTRACT: This paper presents a comprehensive study of the unloading relaxation, damage fracture, and degradation of the mechanical parameters of surrounding rocks in underground caverns during excavation using acoustic velocity test, borehole camera test, and borehole elastic modulus test. First, the range of excavation damaged zone is determined by the results of acoustic velocity test. Then, from borehole camera images, information of the distribution and evolution of fissures and cracks during blasting excavation is obtained. Finally, the relationship between elastic modulus and acoustic velocity is established by the borehole elastic modulus tests and acoustic velocity results. The mechanical parameters of the excavation damaged zone and surrounding undisturbed rocks of underground caverns are directly determined by *in situ* geophysical and geotechnical tests. It provides a direct basis for feedback analysis of displacement monitoring and advanced deformation forecasting of surrounding rocks in underground caverns.

1 INTRODUCTION

Excavation damaged zone of the surrounding rock is a key science question on rock mechanics and construction site design. Through *in situ* geophysical and geotechnical tests, unloading relaxation, damage fracture, and degradation of the mechanical parameters of surrounding rocks during excavation can be obtained directly and efficiently. Scientists have made several achievements on *in situ* geophysical and geotechnical tests on the excavation damaged zone.

Anderson et al. (2009) carried out several experiments in the Hard Rock Laboratory on the Sweden Äspö Island. Yan et al. (2009) studied the damage characteristics of surrounding rocks for tunnels constructed using TBM and drill and blast. Li et al. (2010) conducted tests on the formation and evolution of TBM excavation damaged zone in deep-buried tunnel based on the digital panoramic borehole camera technique. Liu et al. (2011) detected and analyzed the excavation damaged zone of deep tunnel by means of acoustic test, drilling TV, and numerical methods. Zhang et al. (2011) analyzed a large number of velocity–depth curves and proposed an acoustic velocity fitting of the excavation damaged zone of surrounding rock in underground powerhouse. Dai et al. (2015) used acoustic wave test, borehole TV, and micro-seismic monitoring to study the characteristics of damaged zones due to excavation in deep underground powerhouse at Houziyan hydropower station.

Previous research works are mainly based on a single method, such as acoustic testing, micro-seismic monitoring, borehole elasticity modulus, and borehole camera, to evaluate the evolution of excavation damaged zone of underground engineering surrounding rock. It rarely combines with different types of testing methods. In this paper, a hydroelectric station underground power house is chosen for the case study. *In situ* geophysical and geotechnical tests of surrounding rock on the construction phase are conducted. Unloading relaxation, damage fracture, and degradation of the mechanical parameters of surrounding rocks during excavation are studied. It provides a direct basis for feedback analysis of displacement monitoring and advanced deformation forecasting of surrounding rocks in underground caverns.

2 METHODS

2.1 *Acoustic velocity test*

Single-borehole acoustic test uses single-emitting with double-receiving energy converters in the borehole. The outside equipment is composed of the pulse signal source and recording device, as shown in Figure 1. Water is used as coupling agent and test point spacing is 20 cm. Rock acoustic velocity V_P is calculated as follows:

$$V_P = \frac{L}{(t_2 - t_1)} \tag{1}$$

where L is the distance between two receiving energy converters and t_2 and t_1 are the arrival times of the second and first waves, respectively.

2.2 *Borehole camera test*

Digital borehole camera is composed of hardware part and image processing system. The hardware part includes winch, panoramic probe, control box, equipment box, camcorder, desktop computers, and other components that receive real-time information from the downhole probe. According to image orientation information, an image processing system expands each image in the order of NESW and then stitches together to a full-borehole expanded-view image, as shown in Figure 1b. The circular accuracy of the digital borehole camera is up to 0.1–0.2 mm.

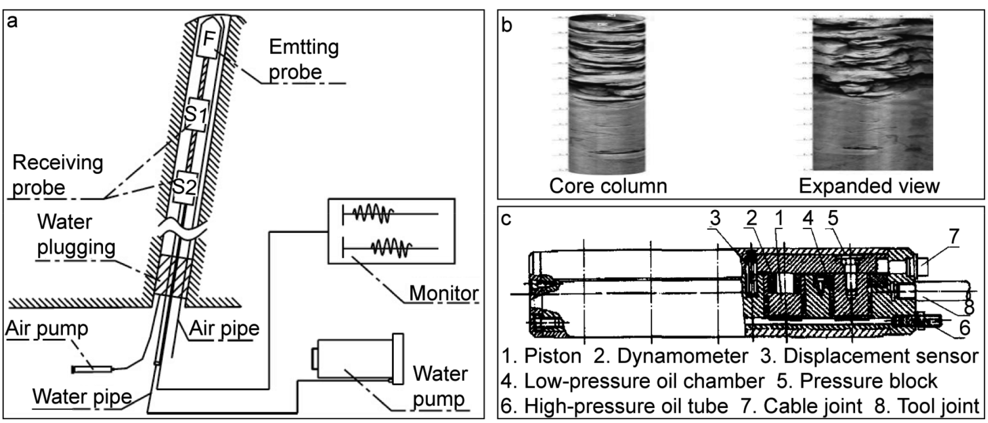

Figure 1. Schematic diagram of single-borehole acoustic test; b. Images of borehole camera; c. Schematic diagram of borehole dilatometer.

2.3 *Borehole elastic modulus tests*

Borehole elastic modulus test uses four internal pistons pushing two rigid bearing plates in borehole dilatometer, which applies symmetrical strip loads on the borehole wall rock, as shown in Figure 1c. The elastic modulus (E) of test site rock is calculated as follows:

$$E = A \times H \times D \times T(\nu, \beta) \times \frac{\Delta Q}{\Delta D} \tag{2}$$

where A is the influence coefficient of two-dimensional calculation formula considering three-dimensional problem; H is the hydraulic correction coefficient of dilatometer; D is the borehole diameter; T(ν, β) is the coefficient determined by rock Poisson ratio and angle of circumference of bearing plate; ΔQ is load increment; and ΔD is deformed increment.

2.4 *Determination of the excavation damaged zone*

At present, the excavation damaged zone of rock has no uniform definition and measuring method. There are two methods to determine the excavation damaged zone of rock in engineering practice:

1. The area of borehole acoustic velocity is significantly reduced, thereby determining the range of the excavation damaged zone.
2. Determining the area of significant change in the physical and geotechnical properties of rock, including rupture, stress redistribution, and elastic modulus.

In this paper, acoustic velocity and borehole camera methods are comprehensively used to determine the excavation damaged zone of rock in underground caverns.

3 CASE STUDY

3.1 *Engineering background*

The hydroelectric station underground caverns used as case study include main power house, transformer chamber, and tailrace surge chamber, which are arranged in parallel and in the axial direction of NE50° with spacing of 41.5 m and 35.5 m. The outline dimensions of the three main caverns are 189 m × 26.7 m × 70.25 m (length × width × height), 143.7 m × 18.0 m × 34.3 m, and 116.50 m × 20.0 m × 65.9 m, as shown in Figure 2. The vertical burial depth is in the range of 129–331 m and the lateral burial depth is 124–154 m. The lithology of the underground cavern is layered or laminated sandstone and slate.

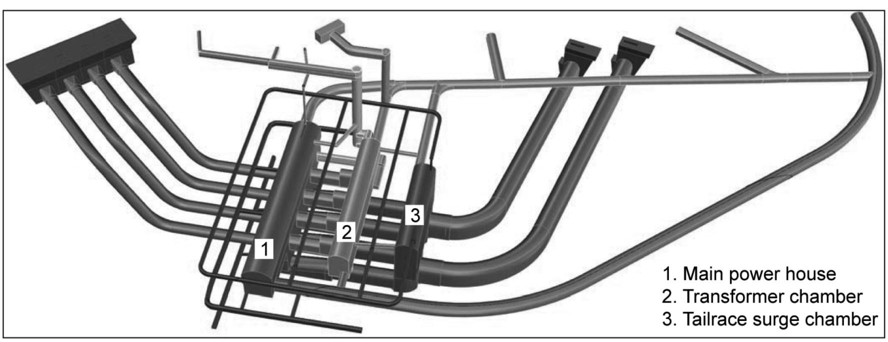

Figure 2. Layout of the hydroelectric station underground caverns.

3.2 *Monitoring scheme*

In order to reflect the relaxation processes and structure revolution of rocks in different lithologies in the process of excavation, boreholes are respectively drilled in sandstone and slate. Along the longitudinal axis of the three underground caverns, four rows of boreholes are arranged. Figure 3 shows the second row of physical boreholes. The diameter of the physical borehole is 76 mm and the depths of the boreholes are in the range of 25–48 m.

3.3 *The range of excavation damaged zones of caverns*

With acoustic velocity as the evaluation criterion for excavation damaged zone, the ranges of excavation damaged zone of the three underground caverns are obtained, as shown in Figures 4 and 5. Table 1 shows the results of geophysical and geotechnical tests of main power house. The range of average acoustic velocity is 4.31–4.74 km/s. The average elastic modulus ranges from 10.38 to 13.2 GPa, while the average deformation modulus ranges from 8.5 to 10.23 GPa. Comparing with other caverns, the main power house has the largest excavation span with 26.7 m. The downstream sidewall of main power has the deepest excavation damaged zone ranging from 1.2 to 4.6 m. The lengths of anchor in the support system of underground caverns are respectively 6 and 9 m, which can effectively limit the deformation of the surrounding rock.

3.4 *Relationships between the results of geophysical and geotechnical tests and depth*

Figure 5 shows the change of borehole acoustic velocity, elastic modulus, deformation modulus, and cracks with depth in the borehole C2-2. The fluctuation of physical properties has good correspondence with borehole cracks. This shows that physical properties in the crack area abruptly decrease. Furthermore, the deterioration of physical properties is higher in large crack.

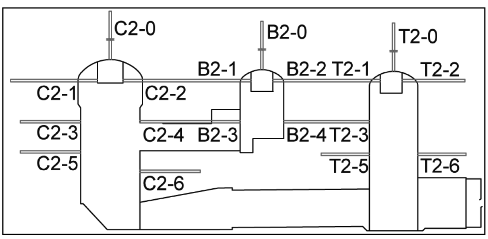

Figure 3. Layout of the physical boreholes.

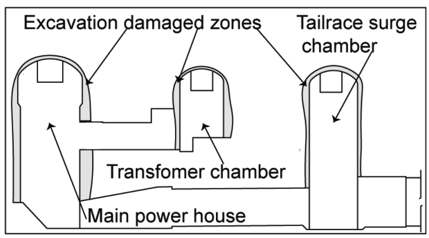

Figure 4. Excavation damaged zones of caverns.

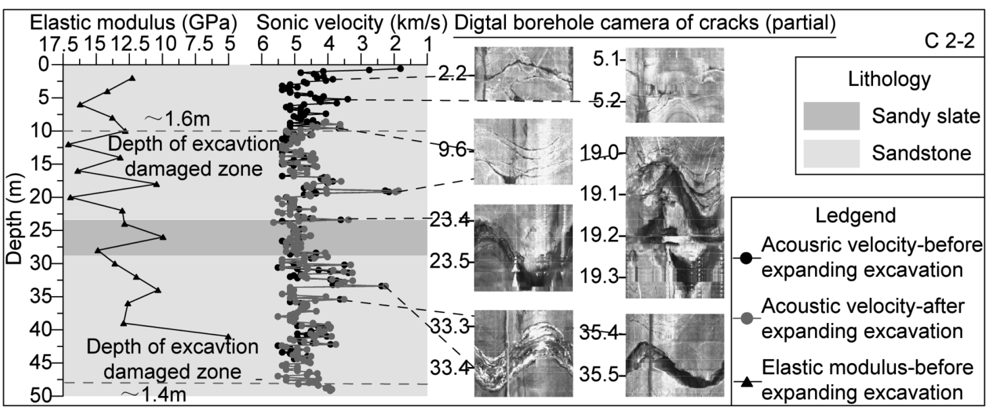

Figure 5. Geophysical test results of borehole C2-2.

Table 1. Geophysical and geotechnical test results of the main power house.

Location	Core No.	Acoustic velocity (km/s)	Elastic modulus (GPa)	Deformation modulus (GPa)	Excavation damaged zone (m)
Main power house	C2-0	/	12.05	9.72	/
	C2-1	4.56	11.23	8.7	1.2
	C2-2	4.74	13.02	8.97	1.6
	C2-3	4.38	11.45	9.37	3.4
	C2-4	4.39	11.9	9.47	4.6
	C2-5	4.67	10.38	8.5	3
	C2-6	4.31	13.2	10.23	1.6

Acoustic velocity, elastic modulus, and deformation are average values.

Table 2. Comparison of acoustic velocity between excavation damaged zone and undisturbed area.

Core No.	Undisturbed area (km/s)				Excavation damaged zone (km/s)				Decrement (km/s)	Attenuation ratio (%)
	Max.	Min.	Ave.	SD	Max.	Min.	Ave.	SD		
C1-2	5.64	2.27	4.81	0.60	5.26	1.92	4.03	0.91	0.78	16.28
C2-1	5.64	1.81	4.57	0.63	4.21	3.73	4.05	0.19	0.52	11.42
C2-2	5.64	2.16	4.78	0.56	5.14	1.81	4.09	0.86	0.69	14.44
C4-1	5.78	2.67	4.48	0.58	4.56	2.16	3.82	0.71	0.66	14.67

Max., maximum value; Min., minimum value; Ave., average value; SD, standard deviation.

3.5 *Comparison of acoustic velocity between excavation damaged zone and undisturbed area*

The results of acoustic velocity between excavation damaged zone and undisturbed area are shown in Table 2. The average acoustic velocity of undisturbed area ranges from 4.21 to 5.14 km/s, whereas the average acoustic velocity of excavation damaged zone ranges from 2.94 to 5.05 km/s. The average attenuation ratio of excavation damaged zone ranges from 11.42 to 16.28%.

4 DISCUSSION

4.1 *Influence of expanding excavation on the physical properties of rock*

Before and after the first-layer expanding excavation, borehole acoustic velocity test and camera test were conducted on four boreholes. The results of comparison of acoustic velocity between before and after first-layer expanding excavation are shown in Table 3. The results of the acoustic velocity test show that the attenuation ratio of acoustic velocity ranges from 1.66% to 2.51% in the impact of the first-layer blasting expanding excavation.

Figure 6 shows the crack evolution processes before and after expanding excavation. A number of irregular slight cracks are developed in the 0.00–0.10 m part of borehole C2-1 located at the upstream sidewall of main power house after first-layer expanding excavation. A similar situation is found in the 0.00–0.10 m and 1.0–1.1 m parts of borehole C4-1 at the upstream sidewall of the main power house. No new cracks are found in the remaining parts of boreholes due to the impact of the first-layer blasting expanding excavation. In general, the effect of the first-layer blast expanding excavation on crack growth and the physical properties of underground cavern rock is not significant.

4.2 *Relationship between acoustic velocity and elastic modulus*

Similarly to acoustic velocity, elastic modulus of rock is influenced by the crack development characteristics. Thus, these two parameters have good correspondence.

Exponential fitting between acoustic velocity and elastic velocity is established using the least squares method. The relationships between acoustic velocity and elastic modulus of sandstone and slate are obtained, as shown in Figure 7.

The results indicate that the relationships between elastic modulus and acoustic wave velocity have low correlation coefficient, in the range of 0.45–0.48. The potential reason is that a number of cracks and fissures exist on the wall of boreholes. On the one hand, when high dip angle cracks exist, the direction of propagation of acoustic wave is approximately parallel to the direction of cracks. The acoustic velocity decreases slightly, while the elastic modulus is more susceptible to the high dip angle cracks. Therefore, high acoustic velocity is achieved with low elastic modulus. On the other hand, when low dip angle cracks exist, the direction of propagation of acoustic wave is approximately perpendicular to the direction of cracks. The acoustic velocity decreases sharply, while the elastic modulus is less susceptible to the low dip angle cracks. Therefore, low acoustic velocity is achieved with high elastic modulus. In general, the direction of crack has a direct effect on the correlation between acoustic velocity and elastic modulus.

Table 3. Comparison of acoustic velocity between before and after first-layer expanding excavation.

Core No.	Before expanding excavation (km/s)				After expanding excavation (km/s)				Decrement (km/s)	Attenuation ratio (%)
	Max.	Min.	Ave.	SD	Max.	Min.	Ave.	SD		
C1-2	5.64	2.27	4.81	0.58	5.64	1.98	4.71	0.64	0.10	2.02
C2-1	5.64	1.81	4.59	0.65	5.44	1.71	4.48	0.64	0.11	2.37
C2-2	5.64	2.16	4.79	0.57	5.64	1.87	4.67	0.62	0.12	2.51
C4-1	5.78	2.67	4.48	0.60	5.78	2.63	4.40	0.58	0.08	1.66

Max., maximum value; Min., minimum value; Ave., average value; SD, standard deviation.

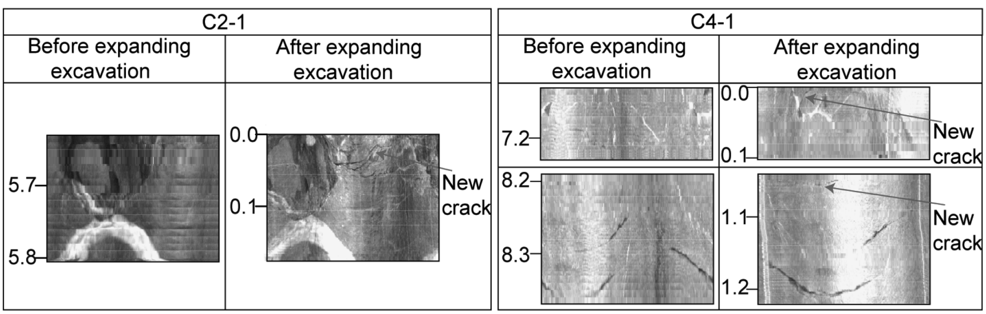

Figure 6. Borehole camera images of crack evolution process before and after expanding excavation.

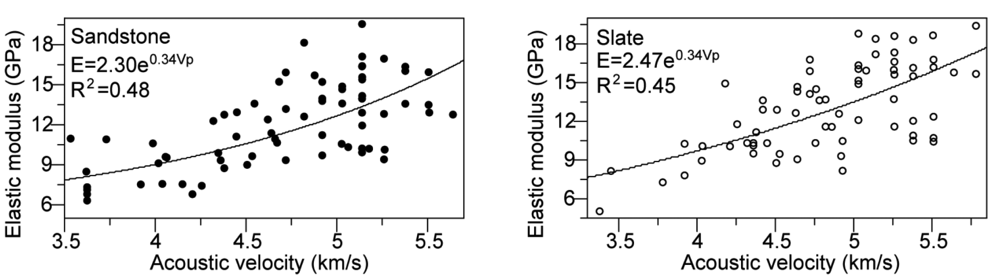

Figure 7. Relationships between acoustic velocity and elastic modulus of sandstone and slate.

5 CONCLUSIONS

In summary, integrating acoustic velocity test, borehole camera test, and borehole elastic modulus test have been used to study the unloading relaxation, damage fracture, and degradation of the mechanical parameters of surrounding rocks in underground caverns. The following conclusions can be drawn:

– The fluctuation of physical properties has good correspondence with borehole cracks. Physical properties abruptly deteriorate in the crack region.
– The damaged zone of underground caverns ranges from 1.2 to 4.6 m. The anchor support system can effectively limit the deformation of the surrounding rock.
– The average attenuation ratio of acoustic velocity in excavation damaged zone ranges from 11.42% to 16.28%.
– The effect of the first-layer blast expanding excavation on the crack growth and physical properties of underground cavern rock is not significant.
– The direction of crack has a direct effect on the correlation between acoustic velocity and elastic modulus.

ACKNOWLEDGMENTS

The authors gratefully acknowledge the support by the National Key Research and Development Project of China (Grant No. 2016YFC0401802), the State Key Program of National Natural Science of China (Grant No. 51539002), and the National Natural Science Foundation of China (Nos. 51209198 and 51204158).

REFERENCES

Anderson, J.C., C.D. Martin. 2009. The Aspo pillar stability experiment: Part I-Experiment design. *International Journal of Rock Mechanics and Mining Sciences* 46(5): 865–878.
Dai et al. 2015. Characteristics of damaged zones due to excavation in deep underground powerhouse at Houziyan hydropower station. *Chinese Journal of Rock Mechanics and Engineering* 34(4): 735–736.
Jianhai Zhang et al. 2011. Acoustic velocity fitting and monitoring feedback analysis of surrounding rock loosing zone in underground powerhouse. *Chinese Journal of Rock Mechanics and Engineering* 30(6): 1191–1197.
Ning Liu, Chunsheng Zhang, Weijiang Zhu. 2011. Detection and analysis of excavation damage zone of deep tunnel. *Rock and Soil Mechanics* 32(Suppl.2): 526–532.
Peng Yan et al. 2009. Study of the damage characteristics of surrounding rocks for tunnels constructed using TBM and drill-and-blast. *China Civil Engineering Journal* 42(11): 121–128.
Shaojun Li et al. 2010. Testing on formation and evolution of TBM excavation damaged zone in deep-buried tunnel based on digital panoramic borehole camera technique. *Chinese Journal of Rock Mechanics and Engineering* 29(6): 1106–1112.